AGU PUBLICATIONS

Geophysical Research Letters

RESEARCH LETTER
10.1002/2017GL072585

Key Points:
- Organic coatings on aerosol particles are shown to undergo heterogeneous oxidation by OH much more rapidly than pure organic particles
- The rate constant describing the reactive loss of particulate organic species is linearly dependent on organic surface area-to-volume ratio
- The loading and composition of morphologically complex organic particles may evolve on faster time scales than previously assumed

Supporting Information:
- Supporting Information S1

Correspondence to:
J. H. Kroll,
jhkroll@mit.edu

Citation:
Lim, C. Y., E. C. Browne, R. A. Sugrue, and J. H. Kroll (2017), Rapid heterogeneous oxidation of organic coatings on submicron aerosols, *Geophys. Res. Lett.*, *44*, 2949–2957, doi:10.1002/2017GL072585.

Received 11 JAN 2017
Accepted 15 MAR 2017
Accepted article online 20 MAR 2017
Published online 31 MAR 2017

Rapid heterogeneous oxidation of organic coatings on submicron aerosols

C. Y. Lim[1], E. C. Browne[2], R. A. Sugrue[1], and J. H. Kroll[1]

[1]Department of Civil and Environmental Engineering, Massachusetts Institute of Technology, Cambridge, Massachusetts, USA, [2]Department of Chemistry and Biochemistry, Cooperative Institute for Research in Environmental Sciences, University of Colorado Boulder, Boulder, Colorado, USA

Abstract Laboratory studies have found that heterogeneous oxidation can affect the composition and loading of atmospheric organic aerosol particles over time scales of several days, but most studies have examined pure organic particles only. In this study, in order to probe the reactivity of organic species confined near the particle surface, the rates and products of the OH-initiated oxidation of pure squalane particles are compared to oxidation of thin coatings of squalane on ammonium sulfate particles. The squalane reaction rate constant shows a linear dependence on the organic surface area-to-volume ratio, with rate constants for coated particles up to 10 times larger than for pure particles. Changes in the carbon oxidation state and fraction of particulate carbon remaining show similar enhancements, implying that heterogeneous oxidation may exhibit a stronger effect on the loadings and properties of organic aerosol than previously estimated from laboratory studies.

1. Introduction

Organic aerosol (OA) makes up a significant fraction of fine particulate matter in the atmosphere [*Zhang et al.*, 2007]. Over the course of its atmospheric lifetime (approximately 5 to 10 days [*Balkanski et al.*, 1993]), OA mass and composition can be affected by chemical aging processes, which in turn can alter the climate- and health-relevant properties of the OA. Heterogeneous oxidation, the reaction of gas-phase oxidants (primarily the hydroxyl radical, OH) with organic molecules in the condensed phase, is one important type of aging, with the potential to affect the optical properties, hygroscopicity, and cloud condensation nucleus (CCN) activity of particulate matter [*Cappa et al.*, 2011; *Harmon et al.*, 2013; *Slade and Knopf*, 2014]. Heterogeneous oxidation experiments using a variety of OA proxies, from reduced organic species (alkanes) to highly oxidized organic compounds, generally show increasing average particle carbon oxidation state and loss of particle-phase carbon mass with increasing photochemical age (i.e., OH exposure) [*Kroll et al.*, 2009, 2011; *Smith et al.*, 2009; *Kessler et al.*, 2010, 2012; *Nah et al.*, 2013, 2014; *Chan et al.*, 2014]. Recently, from a reanalysis of a series of flow tube OH oxidation experiments, *Kroll et al.* [2015] estimated that over the course of 1 week, heterogeneous oxidation causes organic particles to lose on average 3–13% of particle-phase carbon and undergo an increase in average carbon oxidation state of 0.2–0.7. These changes are in qualitative agreement with other flow tube heterogeneous oxidation studies on laboratory-generated particles [*George et al.*, 2007; *McNeill et al.*, 2008; *Lambe et al.*, 2011] but are in contrast to results from experiments performed on monolayer films, which showed extremely rapid mass loss with oxidation [*Molina et al.*, 2004].

In order to quantify the importance of heterogeneous oxidation, previous studies have focused on the reactive OH uptake coefficient (γ_{OH}), defined as the fraction of OH-particle collisions that results in reaction. Most studies have found values of γ_{OH} spanning 0.1 to 1 (in the absence of secondary chemistry), indicating efficient oxidation of organic species at particle surfaces [*George and Abbatt*, 2010]. However, the rate at which the composition of an entire organic particle changes depends not only on the rate of reaction at the particle surface but also on the total amount of organic material within the particle (since the material in the interior of the particle must also undergo reaction if the bulk composition of the OA is to change). Assuming that mixing within the particle (i.e., the diffusion of material from the particle interior to the surface) is rapid, the second-order reaction rate constant (k^{II}) of a parent organic compound in the particle phase is equal to the oxidant flux to the particle surface divided by the number of parent molecules present in the particle:

$$k^{II} = \frac{\gamma_{OH} \cdot \bar{c} \cdot M_w \cdot SA}{4 \cdot N_A \cdot \rho_0 \cdot V} \quad (1)$$

in which γ_{OH} is the reactive uptake coefficient, $\bar{c}$ is the mean molecular speed of the gas-phase oxidant, N_A is Avogadro's number, ρ_0 and M_w are the density and molecular weight, respectively, of the reactive organic compound, *SA* is the surface area of the organic component available for reaction on the particle surface, and *V* is the volume of the organic component of the particle. This rate constant refers not to the elementary OH-organic reaction at the molecular level, but instead to the reaction between gas-phase OH and generic organic species within the particle [*Smith et al.*, 2009]. Assuming a well-mixed spherical particle, equation (1) simplifies to

$$k^{II} = \frac{3 \cdot \gamma_{OH} \cdot \bar{c} \cdot M_w}{2 \cdot N_A \cdot \rho_0 \cdot D_S} \quad (2)$$

where D_s is the particle surface weighted diameter. Estimates of particle oxidation lifetimes with respect to OH ($\tau = 1/(k^{II}[OH])$) using this relationship are on the order of days to weeks—significant for the composition of particles during long-term aging, but unlikely to affect the composition or mass of OA on shorter time scales [*Robinson et al.*, 2006; *Kroll et al.*, 2015].

However, the assumption that OA particles are spherical and well-mixed is a major simplification; field observations and laboratory experiments have shown that atmospheric particles are often composed of multiple components and adopt complex morphologies and shapes, such as core-shell, lensed, and fractal [*Li et al.*, 2003; *Fu et al.*, 2012]. These more complex morphologies may have a significant impact on the rates of chemical aging. For example, organic material that condenses and forms a coating on a pre-existing particle (e.g., black carbon or dust) can have an organic SA/V much higher than the SA/V of the total particle. In addition, glassy or diffusion-limited particles [*Koop et al.*, 2011] can have a much higher effective SA/V compared to the particle as a whole, because only the organic species at or near the particle surface are exposed to OH (which has a short reacto-diffusive length in organic phases [*Hanson et al.*, 1994; *Worsnop*, 2002; *Lee and Wilson*, 2016]), while the species within the particles, which cannot diffuse rapidly to the surface, are essentially shielded from reaction. Despite the likely importance of such morphologically complex OA particles in the atmosphere, there have been no systematic studies of organic SA/V on the rates and products of heterogeneous oxidation.

Here we present a flow tube study of the OH-initiated heterogeneous reaction of particles composed of a thin layer of hydrocarbon condensed onto an inorganic seed. This system serves as a model for OA coated on primary particles (e.g., black carbon and dust) and can also serve as a proxy for diffusion-limited particles where oxidation is limited to a thin surface layer. These results are compared to the oxidation of pure organic particles, in order to investigate how organic SA/V controls the kinetics and products of heterogeneous oxidation, providing insight into how this effect impacts predictions of OA mass and composition upon aging.

2. Methods

2.1. Oxidation Flow Reactor Experiments

Experiments involve the heterogeneous oxidation of two particle types: (1) pure, liquid organic aerosol particles and (2) mixed-composition aerosol, composed of a thin organic coating on solid, inorganic seed particles. For both particle types, the organic compound used is squalane (Sigma-Aldrich 99%), which has been used as a model system in previous heterogeneous oxidation studies [*Kroll et al.*, 2009; *Smith et al.*, 2009]. Pure squalane particles were homogeneously nucleated in a tube furnace [*Smith et al.*, 2009], producing nearly lognormal particle distributions (170 nm at 130°C and 215 nm at 145°C). Coated particles were generated by atomizing a solution of ammonium sulfate, drying, then coating the seed particles (~200 nm surface-weighted diameter) with squalane following a similar approach to those found in *Kwamena et al.* [2004] and *Lee and Wilson* [2016]. The amount of squalane condensed onto the seed was controlled by varying the coating temperature between 80°C and 88°C. This produced an increase in measured organic mass but not particle number, indicating that squalane was condensing onto the seed particles with no new particle formation. Additional details on the particle generation techniques are provided in the supporting information.

Oxidation experiments were performed in a type-219 quartz flow tube reactor (130 cm long, 2.5 cm inner diameter); the experimental setup is shown in Figure S1 in the supporting information. The flow tube was run under atmospheric pressure and steady state conditions, with a calculated residence time of 23 s. Dry air

(0.5 standard liters per minute, SLPM) was combined with flow containing particles (0.3 SLPM), ozone (0.3 SLPM) from an ozone generator (Jelight Model 600), humidified air (0.6 SLPM), and the OH-tracer isopentane (150 ppb). Two UV lamps (254 nm, UVP, LLC. XX-40S) were used to photolyze ozone and produce $O(^1D)$, which reacts with water vapor to generate OH radicals and initiate oxidation chemistry. OH exposure was varied by changing the concentration of ozone in the flow tube. Photolysis by 254 nm light and oxidation by other species, such as $O^1(D)$ and $O(^3P)$, are likely minor under the reaction conditions used here [*Peng et al.*, 2016]. Temperature in the flow tube enclosure was regulated by rapid airflow and remained within a few degrees of ambient temperature (20°C); relative humidity within the flow tube was ~30%, ensuring that the ammonium sulfate cores were always solid.

Size distributions of the particles exiting the reactor were measured by a scanning mobility particle sizer (TSI Scanning Mobility Particle Sizer (SMPS) 3936). A high-resolution time-of-flight aerosol mass spectrometer (AMS, Aerodyne Research Inc.) was used to calculate the particle organic fraction, oxygen-to-carbon ratio (O/C), and hydrogen-to-carbon ratio (H/C) of the aerosol after application of measured relative ionization efficiencies (RIEs) for squalane (5.5), ammonium (3.6), and sulfate (1.0), as well as correction factors for elemental analysis [*Aiken et al.*, 2007, 2008]. Revised elemental analysis corrections [*Canagaratna et al.*, 2015] give somewhat higher H/C and O/C; however, the results of this study are largely unaffected by the choice of correction factors. These data enable the calculation of two key quantities, the average carbon oxidation state ($\overline{OS}_C$) and the fraction of the original carbon mass remaining per particle (f_C) [*Kroll et al.*, 2015].

The organic SA/V was determined from combining size-resolved composition measurements, from the AMS operating in particle time-of-flight mode, with mobility size distributions, measured with the SMPS. These estimates assume that the pure organic particles and ammonium sulfate cores were spherical [*Zelenyuk et al.*, 2006] and that squalane formed uniform coatings on the surface of the ammonium sulfate particles. Details on the SA/V calculation are provided in the supporting information. Calculated average organic SA/V ratios for the pure squalane experiments are 0.039 nm^{-1} for the 130°C nucleation and 0.031 nm^{-1} for the 145°C nucleation. Calculated average organic SA/V ratios for the coated experiments are substantially higher, 0.42 nm^{-1}, 0.32 nm^{-1}, and 0.26 nm^{-1} for the 80°C, 83°C, and 88°C experiments, respectively. These correspond to average equivalent coating thicknesses of 2 nm, 3 nm, and 4 nm (assuming a 200 nm core); coating thickness thus increases with temperature, as expected. If the particles have a morphology other than core shell (e.g., squalane partially engulfing the core or existing as small "islands" on the surface), then organic SA/V will be somewhat lower than calculated here but will still be substantially higher than for the pure squalane particles.

OH exposure ($[OH] \times t$) was determined by using the mixed-phase relative rate technique described in *Hearn and Smith* [2006]. Isopentane (C_5H_{12}, Airgas) was used as a gas-phase OH tracer, with concentrations determined by filtering a fraction of the outlet flow through a potassium iodide filter, preconcentrating it on an adsorbent trap (Carbotrap 300, Supelco) for 60 s, and measuring by using a gas chromatograph with flame ionization detector (SRI 8610C). OH exposure, calculated by using the 298 K reaction rate coefficient k_{iP+OH} of 3.65×10^{-12} cm^3 $molecules^{-1}$ s^{-1} [*Wilson et al.*, 2006], varied in the reactor from 0 to 4.5×10^{11} molecules cm^{-3} s; assuming an average atmospheric OH concentration of 1.5×10^6 molecules cm^{-3}, this corresponds to 0–80 h of equivalent atmospheric aging.

3. Results

3.1. Kinetics of Squalane Loss by Heterogeneous Oxidation

The kinetics of the oxidative loss of squalane are shown in Figure 1. Measurement of $C_8H_{17}^+$ was used to monitor the reactive loss of squalane, as this fragment ion has been shown to be an excellent squalane tracer, with no apparent interference from product species [*Smith et al.*, 2009]. The measured rate constant is significantly faster for the coated particles. Exponential fits to the concentration of squalane as a function of OH exposure, shown in Figure 1a, give the second-order squalane rate constant due to reaction with OH (k_{Sq}, equivalent to k^{II} in equation (1)):

$$\frac{[Sq]}{[Sq]_0} = \exp\left(-k_{Sq}\langle OH\rangle \cdot t\right) \tag{3}$$

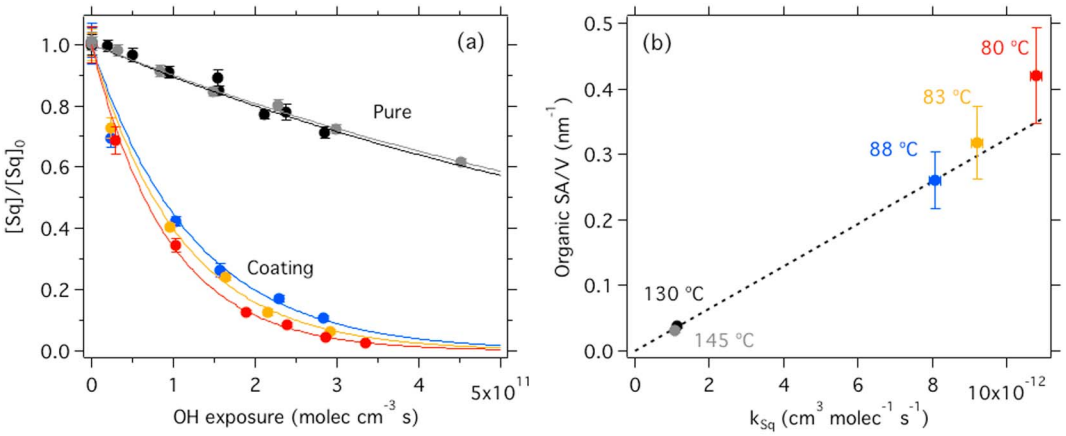

Figure 1. (a) Fraction of squalane remaining as a function of OH exposure. The error bars are 1σ variation in the measurements; the curves are error-weighted exponential fits to the data. The coated particles (80°C, 83°C, and 88°C) show a dramatic increase in the squalane rate constant compared to the pure squalane particles (130°C and 145°C). (b) Organic surface area to volume ratio (nm^{-1}) plotted against squalane rate constant (k_{Sq}, determined from the exponential decay of squalane) for both pure and coated experiments. The dashed line denotes the error-weighted fit to the data, forced through zero.

Measured values of k_{Sq} as a function of organic SA/V are shown in Figure 1b. Compared to the pure squalane experiments, the coated squalane rate constants are enhanced by factors of 7–10. The lowest temperature (i.e., highest organic SA/V) coating corresponds to the greatest enhancement in k_{Sq}. In the coated experiments, k_{Sq} at the lowest OH exposures is somewhat more rapid than at higher OH levels. This may be due to changes in the density, viscosity, or AMS RIE of the particulate organic species upon oxidation, similar to the "leveling off" effect seen in other heterogeneous oxidation experiments [*Kroll et al.*, 2015]. This deviation from the exponential fit is not seen for pure squalane particles until much higher OH exposures not accessed in this experiment, likely due to the much larger reservoir of squalane molecules in the pure organic case.

As shown in Figure 1b, the measured squalane rate constant is proportional (within error) to the organic SA/V of the particles, as predicted by equation (1). We conservatively estimate the average organic SA/V for the coating experiments to be accurate to within ±20% due to uncertainties in the measured relative ionization efficiency for squalane, ammonium, and sulfate, assuming a core-shell morphology. As noted above, it is possible that the particles may be of different shapes and hence have somewhat different organic SA/V than the spherical core-shell morphologies assumed here. However, regardless of their exact configuration, the coated particles certainly have higher organic SA/V than the pure particles, which should lead to an enhancement in the squalane rate constant.

3.2. Changes to Aerosol Chemical Composition

Consistent with the squalane rate constants in Figure 1, the rates of change in the ensemble properties of the particles are also strongly dependent on organic SA/V. Changes to the ensemble chemical composition of OA are quantified in terms of their average carbon oxidation state ($\overline{OS}_C = 2\,O/C - H/C$) and the fraction of carbon mass remaining (f_C) [*Kessler et al.*, 2012; *Kroll et al.*, 2015] and are shown as a function of OH exposure in Figures 2a and 2b. Changes to $\overline{OS}_C$ and f_C are the result of the competition between the addition of oxygenated functional groups (functionalization) and the cleavage of carbon-carbon bonds and potential loss of volatile compounds to the gas phase (fragmentation). The relative importance between these two pathways depends on the molecular makeup of the OA, with fragmentation increasing in importance as molecules become more oxidized [*Kroll et al.*, 2009]. At the highest OH exposures studied, the pure squalane particles show a +0.2 change in $\overline{OS}_C$ and a 10% ± 3% loss of carbon mass. These changes are somewhat faster than those observed by *Smith et al.* [2009], although we calculate identical uptake coefficients (within error); the reason for this is unclear, but is possibly due to differences in reaction conditions (e.g., temperature, relative humidity, and OH concentration). For coated particles, the rate of change in $\overline{OS}_C$ is greatly enhanced compared to the pure experiments, with coatings undergoing up to a +1.3 change in $\overline{OS}_C$. The rate of carbon

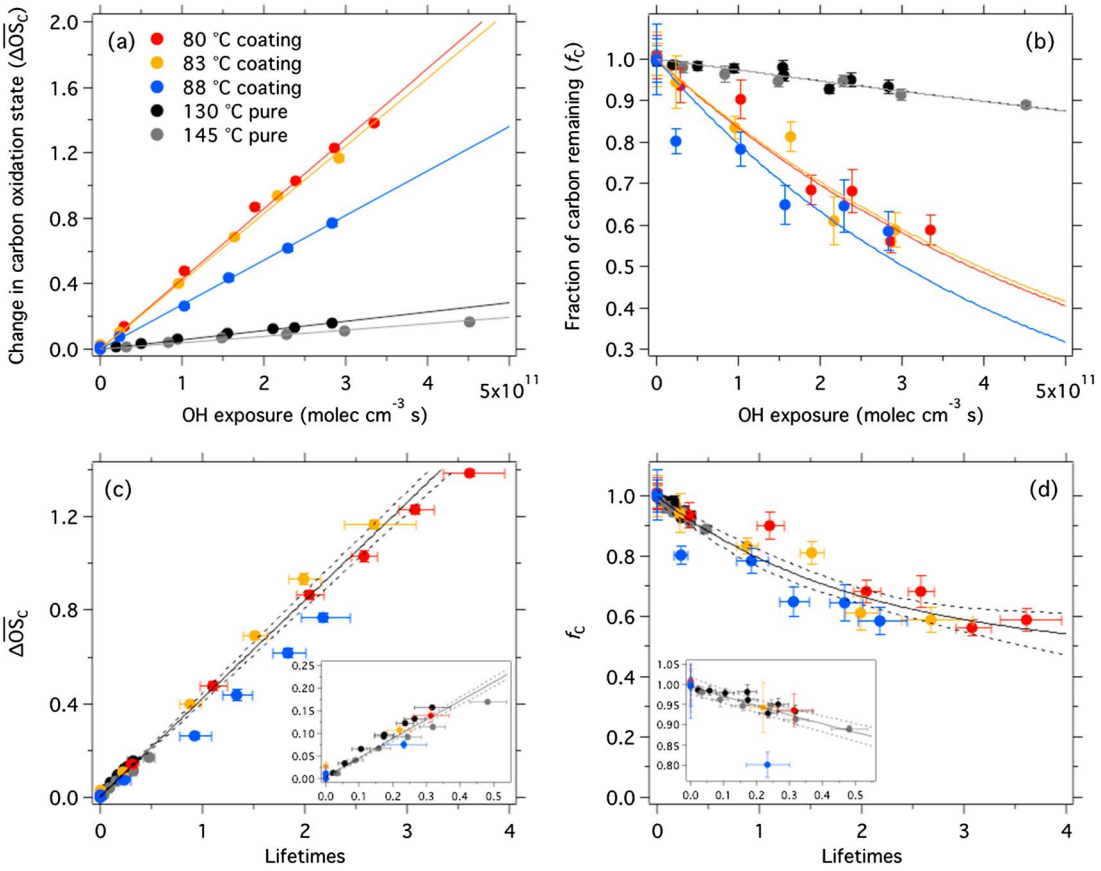

Figure 2. Changes to ensemble chemical properties of the particles upon heterogeneous oxidation. (a) Change in average carbon oxidation state ($\Delta\overline{OS}_C$) as a function of OH exposure. (b) Fraction carbon remaining (f_C) versus OH exposure. The error bars (1σ) are from variability in O/C, H/C, and organic mass measurements. The curves shown are error-weighted fits (linear in Figure 2a, exponential in Figure 2b) to the measurements for each particle type. (c) $\Delta\overline{OS}_C$ and (d) f_C versus squalane lifetimes. The solid lines are error-weighted fits, and the dashed lines represent 95% confidence intervals. The insets show data from 0 to 0.5 lifetimes. Data from all experiments fall on the same line (within experimental error), indicating that changes in ensemble aerosol properties are driven by organic SA/V, rather than differences in chemistry.

loss for coated particles is also enhanced, with losses up to 60% ± 10% of carbon mass. This amount of carbon loss occurs over a relatively short time scale, equivalent to just 2.7 days of atmospheric OH aging (assuming [OH] of 1.5×10^6 molecules cm^{-3}). For comparison, for pure squalane particles to be oxidized to the extent observed for the coated particles, OH exposures equivalent to roughly 30 days of atmospheric processing would be required.

While changes to the ensemble properties of the coated particles are dramatically faster than the changes seen for the pure particles, a linear dependence of $\Delta\overline{OS}_C$ and f_C on organic SA/V is less clear. For example, the rate of change in $\overline{OS}_C$ for the 88°C (thickest) coating is the slowest among the coated experiments, as expected; however, the 80°C and 83°C coatings look very similar. Fluctuations in the organic mass measurements introduce relatively large errors to f_C, possibly masking subtle changes in the rate of carbon mass loss. In order to assess whether the differences in the rates of change for ensemble properties are consistent with the differences in reaction rate constants (k_{sq}), Figures 2c and 2d show $\Delta\overline{OS}_C$ and f_C as a function of oxidation lifetimes (calculated from squalane rate constants, as in *Kroll et al.* [2015]) rather than OH exposure. Describing the ensemble chemical composition in this way allows for chemical changes to be compared on a per-OH reaction basis, independent of differences in physical properties (e.g., SA/V, density, and viscosity). In all experiments (coated and pure), $\Delta\overline{OS}_C$ and f_C exhibit the same dependence on squalane lifetimes (within error). This indicates that the product formation (as described by the ensemble properties $\Delta\overline{OS}_C$ and f_C) is essentially the same in all cases and that the observed differences between the squalane coatings and

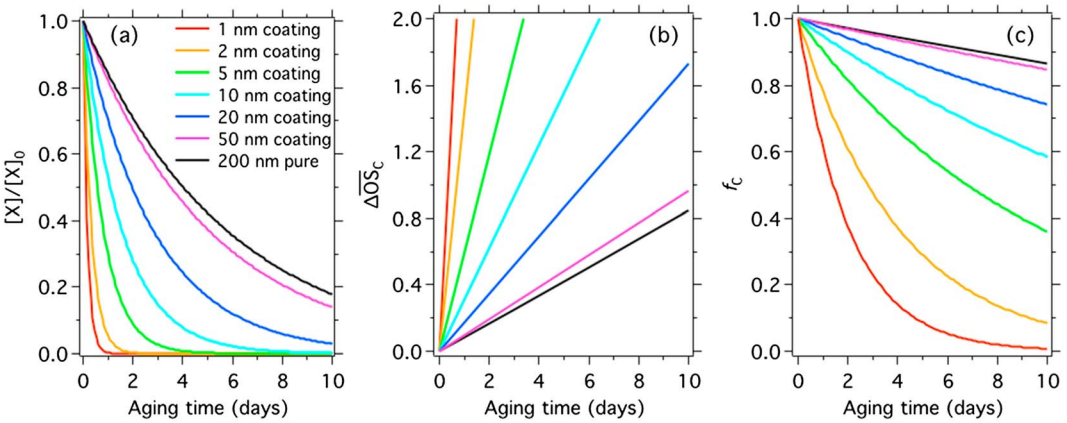

Figure 3. Changes to particle composition due to heterogeneous oxidation for 200 nm particles of different compositions. (a) Fractional loss of an OA component ($[X]/[X]_0$) based on equation (1), (b) change in average carbon oxidation state ($\Delta\overline{OS}_C$), and (c) fractional loss of particle-phase carbon mass (f_C), over 10 days of atmospheric exposure. Figure 3a requires an assumption of the average carbon chain length for the OA component (X) and is assumed to be 10 in this case. Figures 3b and 3c use the heterogeneous oxidation parameterizations from *Kroll et al.* [2015], modified for use with organic coatings.

pure squalane particles are driven by differences in organic SA/V, rather than differences in the underlying kinetics or mechanism of the oxidation reactions themselves.

4. Discussion and Conclusions

We have shown that the heterogeneous transformation of thin organic coatings on particles can be dramatically faster than that of pure organic particles, which are typically used as model systems in laboratory studies of heterogeneous oxidation. This enhancement in the reaction rate constant is driven by differences in the SA/V of the organic fraction of the particle, as expected from equation (1). Such an enhancement is not unique to coated particles but is simply a result of the high organic SA/V; this is in agreement with the trend seen for oxidation of pure palmitic acid particles of varying sizes by *McNeill et al.* [2008]. This means that a small, pure particle will be chemically transformed at the same rate as a thinly coated one (with an inert core), assuming an equivalent organic SA/V. For example, a 2 nm organic coating on a 200 nm core (80°C coating case) has an organic SA/V of 0.42 nm and would be oxidized at the same rate as a pure organic particle with a diameter of 14 nm. Changes in key chemical properties of the OA ($\Delta\overline{OS}_C$ and f_C) show similarly dramatic enhancements for coatings relative to the pure particles, reaching high oxidation states and losing a substantial amount of carbon over OH exposures equivalent to days of atmospheric oxidation, rather than weeks to months required for pure particles. This comparison of coated and pure particle oxidation highlights the importance of particle morphology (organic SA/V) in heterogeneous oxidation kinetics and product formation. Moreover, it may explain the discrepancy in estimated OA volatilization lifetime seen for heterogeneous oxidation experiments on aerosol particles that showed relatively little mass loss [*George et al.*, 2007; *McNeill et al.*, 2008; *Smith et al.*, 2009] and experiments performed on monolayer films that showed dramatic loss of mass over relatively short time scales [*Molina et al.*, 2004].

In order to assess the importance of this effect on the rate of chemical aging in the atmosphere, we apply our results to a particle with physical properties and composition representative of ambient organic particles. We apply the linear organic SA/V relationship observed in this study (and predicted in equation (1)) to the chemical aging parameterizations made in *Kroll et al.* [2015] (10% particle-phase carbon lost and $\Delta\overline{OS}_C$ of +0.59 after 1 week of atmospheric aging) for a typical pure, organic particle (200 nm diameter, O/C = 0.8, H/C = 1.5, $\rho = 1.5\ g\ cm^{-3}$, and $\gamma_{OH} = 1$) and an average [OH] of 1.5×10^6 molecules cm^{-3}. Plots of the reaction kinetics and changes to the ensemble chemical properties of the particles are shown in Figure 3 for both pure particles and particles made up of inert cores with a range of organic coating thicknesses (1 to 50 nm), all with diameters of 200 nm. Figure 3a shows the reactive loss of a hypothetical well-mixed compound in the particle phase (e.g., a tracer molecule or pollutant of interest) as a function of aging time in the atmosphere. The 50 nm coating exhibits only a minor enhancement in loss rate over the pure particle case. The importance

of the organic SA/V becomes more pronounced for the thinner coatings, which show dramatically faster loss compared to the pure or thickly coated particles. This effect on the heterogeneous oxidation rate constant may have implications for the measurement of tracer species used for source apportionment, such as levoglucosan for biomass burning [*Simoneit et al.*, 1999; *Schauer et al.*, 2001] and hopanes for motor vehicle emissions [*Rogge et al.*, 1993]. Such species present in thin (1–10 nm) coatings will essentially be completely lost within a week or less, assuming no subsequent coatings of secondary aerosol.

The change in average carbon oxidation state ($\Delta\overline{OS}_C$) and fraction of particle-phase carbon remaining (f_C) show similar trends, with the 1–20 nm coatings exhibiting markedly faster rates than the pure and 50 nm coated particles. In terms of $\overline{OS}_C$ (Figure 3b), the predicted rate of change is accelerated for coated particles, which exhibit slopes up to +2.8 per day, whereas the slope for pure particles is much more modest, at +0.08 per day. Particle-phase carbon displays a wide range of lifetimes (Figure 3c), ranging from 2 days for 1 nm coatings to 69 days for pure 200 nm particles. So while heterogeneous oxidation plays a relatively minor role in OA lifetime for pure organic particles, it may play a large part in controlling the particle-phase lifetime of OA with high organic SA/V (i.e., thin coatings), or species preferentially present near the surface [*Browne et al.*, 2015]. Over the atmospherically relevant time scale shown here, heterogeneous oxidation may thus potentially be an important OA mass sink and a route toward highly oxidized materials on particle surfaces. Additionally, the rapid modification of surface properties may lead to efficient formation of CCN, given that CCN activity of OA can be critically sensitive to surface composition [*Ruehl and Wilson*, 2014; *Ruehl et al.*, 2016].

Global chemical transport models generally do not include reactions that take into account the heterogeneous oxidation of OA, or they include highly simplified representations of the process [*Heald et al.*, 2011; *Murphy et al.*, 2012; *Hodzic et al.*, 2016]. This is largely due to the absence of laboratory-based parameterizations that can be easily implemented in atmospheric models. The results from this study show that heterogeneous oxidation can be important for the evolution of aerosol composition [*Kroll et al.*, 2015] but also that organic SA/V is critical to the effective rate and products of such oxidation processes in the atmosphere. Thus, in order to accurately simulate the time scales over which OA particles evolve as a result of heterogeneous oxidation, it may be necessary for chemical transport models to track organic SA/V or some similar parameter (e.g., average coating thickness).

Though this work focuses on phase-separated particles and organic coatings, it also has implications for some purely organic particles. For instance, for diffusion-limited particles in which the characteristic particle mixing time is long relative to oxidation, the chemical composition near the surface will change much more rapidly than the bulk of the particle. Thus, the heterogeneous oxidation of such particles may lead to rapid chemical modification of their surfaces, similar to the coated-particle case described above, which could in turn affect their CCN activity and other surface-related properties. This work adds to an increasing number of studies that have emphasized the dependency of chemical aging on the physical properties of particles, as well as environmental conditions such as relative humidity and temperature [*Shiraiwa et al.*, 2011; *Slade and Knopf*, 2014]. Ultimately, understanding the rates, products, and impacts of heterogeneous oxidation relies critically on an improved understanding of the key physical properties (phase, viscosity, morphology, etc.) of ambient particles under a range of atmospheric conditions.

Acknowledgments

The data for this paper are available upon request from the authors. This was supported by the National Science Foundation under grant CHE-1307664 and the Environmental Protection Agency under grant RD-8350331. This work was carried out under assistance agreement D-8350331 awarded by the U.S. Environmental Protection Agency to MIT. It has not been formally reviewed by EPA. The views expressed in this document are solely those of the authors and do not necessarily reflect those of the Agency. EPA does not endorse any products or commercial services mentioned in this publication. C.Y.L. is also supported by the NSF Graduate Research Fellowship Program, and R.A.S. is supported by the MIT Undergraduate Research Opportunities Program. The authors would like to thank T. Onasch and Aerodyne, Inc. for supplying the tube furnace used in this work and K. Wilson and C. Heald for helpful discussions.

References

Aiken, A. C., P. F. DeCarlo, and J. L. Jimenez (2007), Elemental analysis of organic species with electron ionization high-resolution mass spectrometry, *Anal. Chem.*, *79*(21), 8350–8358.

Aiken, A. C., et al. (2008), O/C and OM/OC ratios of primary, secondary, and ambient organic aerosols with high-resolution time-of-flight aerosol mass spectrometry, *Environ. Sci. Technol.*, *42*(12), 4478–4485.

Balkanski, Y. J., D. J. Jacob, G. M. Gardner, W. C. Graustein, and K. K. Turekian (1993), Transport and residence times of tropospheric aerosols inferred from a global three-dimensional simulation of 210Pb, *J. Geophys. Res.*, *98*, 20,573–20,586, doi:10.1029/93JD02456.

Browne, E. C., J. P. Franklin, M. R. Canagaratna, P. Massoli, T. W. Kirchstetter, D. R. Worsnop, K. R. Wilson, and J. H. Kroll (2015), Changes to the chemical composition of soot from heterogeneous oxidation reactions, *J. Phys. Chem. A*, *119*(7), 1154–1163, doi:10.1021/jp511507d.

Canagaratna, M. R., et al. (2015), Elemental ratio measurements of organic compounds using aerosol mass spectrometry: Characterization, improved calibration, and implications, *Atmos. Chem. Phys.*, *15*(1), 253–272.

Cappa, C. D., D. L. Che, S. H. Kessler, J. H. Kroll, and K. R. Wilson (2011), Variations in organic aerosol optical and hygroscopic properties upon heterogeneous OH oxidation, *J. Geophys. Res.*, *116*, D15204, doi:10.1029/2011JD015918.

Chan, M. N., H. Zhang, A. H. Goldstein, and K. R. Wilson (2014), Role of water and phase in the heterogeneous oxidation of solid and aqueous succinic acid aerosol by hydroxyl radicals, *J. Phys. Chem. C*, *118*(50), 28,978–28,992.

Fu, H., M. Zhang, W. Li, J. Chen, L. Wang, X. Quan, and W. Wang (2012), Morphology, composition and mixing state of individual carbonaceous aerosol in urban Shanghai, *Atmos. Chem. Phys.*, *12*(2), 693–707, doi:10.5194/acp-12-693-2012.

George, I. J., and J. P. D. Abbatt (2010), Heterogeneous oxidation of atmospheric aerosol particles by gas-phase radicals, *Nat. Chem.*, *2*(9), 713–722.
George, I. J., A. Vlasenko, J. G. Slowik, K. Broekhuizen, and J. P. D. Abbatt (2007), Heterogeneous oxidation of saturated organic aerosols by hydroxyl radicals: Uptake kinetics, condensed-phase products, and particle size change, *Atmos. Chem. Phys.*, *7*(16), 4187–4201.
Hanson, D. R., A. R. Ravishankara, and S. Solomon (1994), Heterogeneous reactions in sulfuric acid aerosols: A framework for model calculations, *J. Geophys. Res.*, *99*, 3615–3629, doi:10.1029/93JD02932.
Harmon, C. W., C. R. Ruehl, C. D. Cappa, and K. R. Wilson (2013), A statistical description of the evolution of cloud condensation nuclei activity during the heterogeneous oxidation of squalane and bis(2-ethylhexyl) sebacate aerosol by hydroxyl radicals, *Phys. Chem. Chem. Phys.*, *15*(24), 9615–9679.
Heald, C. L., et al. (2011), Exploring the vertical profile of atmospheric organic aerosol: Comparing 17 aircraft field campaigns with a global model, *Atmos. Chem. Phys.*, *11*(24), 12,676–12,696, doi:10.5194/acp-11-12673-2011.
Hearn, J. D., and G. D. Smith (2006), A mixed-phase relative rates technique for measuring aerosol reaction kinetics, *Geophys. Res. Lett.*, *33*, L17805, doi:10.1029/2006GL026963.
Hodzic, A., P. S. Kasibhatla, D. S. Jo, C. D. Cappa, J. L. Jimenez, S. Madronich, and R. J. Park (2016), Rethinking the global secondary organic aerosol (SOA) budget: Stronger production, faster removal, shorter lifetime, *Atmos. Chem. Phys.*, *16*(12), 7917–7941, doi:10.5194/acp-16-7917-2016.
Kessler, S. H., J. D. Smith, D. L. Che, D. R. Worsnop, K. R. Wilson, and J. H. Kroll (2010), Chemical sinks of organic aerosol: Kinetics and products of the heterogeneous oxidation of erythritol and levoglucosan, *Environ. Sci. Technol.*, *44*(18), 7005–7010.
Kessler, S. H., T. Nah, K. E. Daumit, J. D. Smith, S. R. Leone, C. E. Kolb, D. R. Worsnop, K. R. Wilson, and J. H. Kroll (2012), OH-initiated heterogeneous aging of highly oxidized organic aerosol, *J. Phys. Chem. A*, *116*(24), 6358–6365.
Koop, T., J. Bookhold, M. Shiraiwa, and U. Pöschl (2011), Glass transition and phase state of organic compounds: Dependency on molecular properties and implications for secondary organic aerosols in the atmosphere, *Phys. Chem. Chem. Phys.*, *13*(43), 19,238, doi:10.1039/c1cp22617g.
Kroll, J. H., J. D. Smith, D. L. Che, S. H. Kessler, D. R. Worsnop, and K. R. Wilson (2009), Measurement of fragmentation and functionalization pathways in the heterogeneous oxidation of oxidized organic aerosol, *Phys. Chem. Chem. Phys.*, *11*(36), 8005.
Kroll, J. H., et al. (2011), Carbon oxidation state as a metric for describing the chemistry of atmospheric organic aerosol, *Nat. Chem.*, *3*(2), 133–139, doi:10.1038/nchem.948.
Kroll, J. H., C. Y. Lim, S. H. Kessler, and K. R. Wilson (2015), Heterogeneous oxidation of atmospheric organic aerosol: Kinetics of changes to the amount and oxidation state of particle-phase organic carbon, *J. Phys. Chem. A*, *119*(44), 10,767–10,783.
Kwamena, N. O. A., J. A. Thornton, and J. P. D. Abbatt (2004), Kinetics of surface-bound benzo[a]pyrene and ozone on solid organic and salt aerosols, *J. Phys. Chem. A*, *108*(52), 11,626–11,634, doi:10.1021/jp046161x.
Lambe, A. T., et al. (2011), Characterization of aerosol photooxidation flow reactors: Heterogeneous oxidation, secondary organic aerosol formation and cloud condensation nuclei activity measurements, *Atmos. Meas. Tech.*, *4*(3), 445–461.
Lee, L., and K. Wilson (2016), The reactive-diffusive length of OH and ozone in model organic aerosols, *J. Phys. Chem. A*, *120*(34), 6800–6812, doi:10.1021/acs.jpca.6b05285.
Li, J., M. Posfai, P. V. Hobbs, and P. R. Buseck (2003), Individual aerosol particles from biomass burning in southern Africa: 2. Compositions and aging of inorganic particles, *J. Geophys. Res.*, *108*(D13), 8484, doi:10.1029/2002JD002310.
McNeill, V. F., R. L. N. Yatavelli, J. A. Thornton, C. B. Stipe, and O. Landgrebe (2008), Heterogeneous OH oxidation of palmitic acid in single component and internally mixed aerosol particles: Vaporization and the role of particle phase, *Atmos. Chem. Phys.*, *8*, 5465–5476, doi:10.5194/acp-8-5465-2008.
Molina, M. J., A. V. Ivanov, S. Trakhtenberg, and L. T. Molina (2004), Atmospheric evolution of organic aerosol, *Geophys. Res. Lett.*, *31*, L22104, doi:10.1029/2004GL020910.
Murphy, B. N., N. M. Donahue, C. Fountoukis, M. Dall'Osto, C. O'Dowd, A. Kiendler-Scharr, and S. N. Pandis (2012), Functionalization and fragmentation during ambient organic aerosol aging: Application of the 2-D volatility basis set to field studies, *Atmos. Chem. Phys.*, *12*(22), 10,797–10,816, doi:10.5194/acp-12-10797-2012.
Nah, T., S. H. Kessler, K. E. Daumit, J. H. Kroll, S. R. Leone, and K. R. Wilson (2013), OH-initiated oxidation of sub-micron unsaturated fatty acid particles, *Phys. Chem. Chem. Phys.*, *15*(42), 18,615–18,649.
Nah, T., S. H. Kessler, K. E. Daumit, J. H. Kroll, S. R. Leone, and K. R. Wilson (2014), Influence of molecular structure and chemical functionality on the heterogeneous OH-initiated oxidation of unsaturated organic particles, *J. Phys. Chem. A*, *118*(23), 4106–4119.
Peng, Z., D. A. Day, A. M. Ortega, B. B. Palm, W. Hu, H. Stark, R. Li, K. Tsigaridis, W. H. Brune, and J. L. Jimenez (2016), Non-OH chemistry in oxidation flow reactors for the study of atmospheric chemistry systematically examined by modeling, *Atmos. Chem. Phys.*, *16*(7), 4283–4305, doi:10.5194/acp-16-4283-2016.
Robinson, A. L., N. M. Donahue, and W. F. Rogge (2006), Photochemical oxidation and changes in molecular composition of organic aerosol in the regional context, *J. Geophys. Res.*, *111*, D03302, doi:10.1029/2005JD006265.
Rogge, W. F., L. M. Hildemann, M. A. Mazurek, G. R. Cass, and B. R. T. Simoneit (1993), Sources of fine organic aerosol. 2. Noncatalyst and catalyst-equipped automobiles and heavy-duty diesel trucks, *Environ. Sci. Technol.*, *27*(4), 636–651, doi:10.1021/es00041a007.
Ruehl, C. R., and K. R. Wilson (2014), Surface organic monolayers control the hygroscopic growth of submicrometer particles at high relative humidity, *J. Phys. Chem. A*, *118*(22), 3952–3966, doi:10.1021/jp502844g.
Ruehl, C. R., J. F. Davies, and K. R. Wilson (2016), An interfacial mechanism for cloud droplet formation on organic aerosols, *Science*, *351*(6280), 1447–1450.
Schauer, J. J., M. J. Kleeman, G. R. Cass, and B. R. T. Simoneit (2001), Measurement of emissions from air pollution sources. 3. C1–C29 organic compounds from fireplace combustion of wood, *Environ. Sci. Technol.*, *35*(9), 1716–1728, doi:10.1021/es001331e.
Shiraiwa, M., M. Ammann, T. Koop, and U. Pöschl (2011), Gas uptake and chemical aging of semisolid organic aerosol particles, *Proc. Natl. Acad. Sci. U.S.A.*, *108*, 11,003–11,008, doi:10.1073/pnas.1103045108.
Simoneit, B. R. T., J. J. Schauer, C. G. Nolte, D. R. Oros, V. O. Elias, M. P. Fraser, W. F. Rogge, and G. R. Cass (1999), Levoglucosan, a tracer for cellulose in biomass burning and atmospheric particles, *Atmos. Environ.*, *33*(2), 173–182, doi:10.1016/S1352-2310(98)00145-9.
Slade, J. H., and D. A. Knopf (2014), Multiphase OH oxidation kinetics of organic aerosol: The role of particle phase state and relative humidity, *Geophys. Res. Lett.*, *41*, 5297–5306, doi:10.1002/2014GL060582.
Smith, J. D., J. H. Kroll, C. D. Cappa, D. L. Che, C. L. Liu, M. Ahmed, S. R. Leone, D. R. Worsnop, and K. R. Wilson (2009), The heterogeneous reaction of hydroxyl radicals with sub-micron squalane particles: A model system for understanding the oxidative aging of ambient aerosols, *Atmos. Chem. Phys.*, *9*(9), 3209–3222.

Wilson, E. W., W. A. Hamilton, H. R. Kennington, B. Evans, N. W. Scott, and W. B. DeMore (2006), Measurement and estimation of rate constants for the reactions of hydroxyl radical with several alkanes and cycloalkanes, *J. Phys. Chem. A*, *110*(10), 3593–3604.

Worsnop, D. R. (2002), A chemical kinetic model for reactive transformations of aerosol particles, *Geophys. Res. Lett.*, *29*(20), 1996, doi:10.1029/2002GL015542.

Zelenyuk, A., Y. Cai, and D. Imre (2006), From agglomerates of spheres to irregularly shaped particles: Determination of dynamic shape factors from measurements of mobility and vacuum aerodynamic diameters, *Aerosol Sci. Technol.*, *40*(3), 197–217, doi:10.1080/02786820500529406.

Zhang, Q., et al. (2007), Ubiquity and dominance of oxygenated species in organic aerosols in anthropogenically-influenced Northern Hemisphere midlatitudes, *Geophys. Res. Lett.*, *34*, L13801, doi:10.1029/2007GL029979.